

# Electron bunching in triple quantum dot interferometers

Fernando Domínguez, Gloria Platero, Sigmund Kohler

*Instituto de Ciencia de Materiales de Madrid, CSIC, Cantoblanco, E-28049 Madrid, Spain*

---

## Abstract

We study electron transport through a triple quantum dot in ring configuration at finite bias. In particular, we analyze the influence of a gate voltage that detunes one of the dots, such that one branch of the interferometer becomes off-resonant. It turns out that then interference effects fade away, i.e., the current becomes independent of a penetrating flux and the detuning. The noise properties which are characterized by the full-counting statistics, however, are governed by bunching effects that may be tuned by the gate voltage. Analytical results for limiting cases support this picture. A possible application is the construction of current sources with widely tunable shot noise properties.

*Keywords:* quantum dots, quantum transport, full counting statistics

*PACS:* 73.23.-b, 05.60.Gg, 74.50.+r

---

## 1. Introduction

During the last decade, a huge effort has been made to understand the conduction properties of quantum systems that consist of only a few discrete levels. Spurred by Feynman's vision of "plenty of room at the bottom" [1], it has e.g. been proposed to use single molecules as elements of future electronic circuits [2]. Although this task is far from being accomplished, molecular electronics already became an established field [3, 4]. Apart from their technological promises, conducting molecules may also serve as tools for the implementation of fundamental physical phenomena. One example is the intriguing effect of tunnel suppression by the purely coherent influence of an ac field [5], which is stable even in the presence of Coulomb repulsion [6]. Coherent destruction of tunneling leaves its fingerprints in the transport characteristics of a laser-driven molecular wire, where an ac field may suppress the current and its fluctuations [7, 8, 9, 10].

From a theoretical perspective, molecular wires share many features with quantum dots. In particular, the electronic structure of both systems consists of discrete states. Owing to this fact, coherently coupled quantum dots may be considered as "artificial molecules", despite the fact that their energy scales are several orders of magnitude smaller than those of real molecules. For roughly one decade, the state of the art has been to couple just two quantum dots coherently [11, 12, 13], while coherently coupled triple quantum dots have been realized only recently [14, 15, 16]. Both double quantum dots [17] and triple quantum dots [15, 16] can be constructed such that electron coming from the source may proceed on two different paths towards the drain. There they interfere constructively or destructively, depending on the setup and a possible flux enclosed by the interfering paths. More-

over, there exist dark states which are superpositions that are decoupled from the drain and, thus, block the electron transport [18, 19]. Such blockade may be resolved by excitations with proper ac fields [20, 21].

Here we investigate the conduction properties of a triple quantum dot in ring configuration as sketched in Fig. 1. A penetrating flux allows the operation as Aharonov-Bohm interferometer. We focus on the influence of a gate voltage that allows shifting of the levels of dot 2 out of resonance. The intuitive expectation is that for strong detuning, the two other dots govern the transport process, such that its properties are essentially those of a double quantum dot. While this is indeed the case for the current, electrons temporarily trapped in dot 2 may interrupt the transport. Consequently, the electron flow becomes avalanche-like.

An established theoretical tool for characterizing such correlated transport is full counting statistics [22, 23, 24] which provides the complete information about the distribution of the transported charge in terms of the corresponding cumulants. For a Markovian master equation as employed below, it is possible to express these cumulants as derivatives of a particular eigenvalue of the Liouville operator augmented by a counting variable [23]. Generally, this requires the computation of derivatives of arbitrary high order. As soon as one has to rely on a numerical treatment, practical calculations may represent a formidable task. Recently, Flindt *et al.* have found a way to circumvent this difficulty [25]. Based on Rayleigh-Schrödinger perturbation theory, they derived a scheme that allows one to compute the full counting statistics recursively. We use this approach for our numerical solution.

Our paper is organized as follows. In Section 2 we introduce a system-lead Hamiltonian and derive a master equation formalism for the computation of the full count-

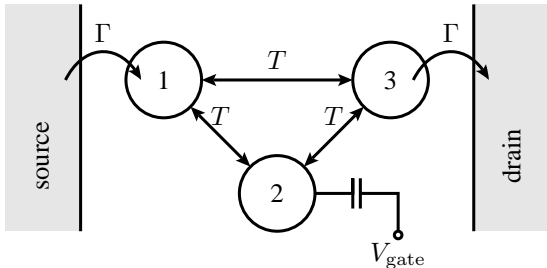


Figure 1: Triple quantum dot in ring configuration coupled to electron source and drain. The onsite energies of dots 1 and 3 are  $\epsilon_{1,3} = 0$ , while the onsite energy of dot 2 can be tuned by a gate voltage such that  $\epsilon_2 = V_{\text{gate}}/e$ .

ing statistics. The numerical results for the current and the zero-frequency noise, presented in Section 3, provide information about the super-Poissonian nature of the transport process. In Section 4, we derive analytical expressions for the cumulants up to fourth order valid in the low-bias regime.

## 2. Model and master equation approach

### 2.1. Dot-lead Hamiltonian

We consider a triple quantum dot with a ring-shaped geometry as depicted in Fig. 1, which is described by the Hamiltonian

$$H_{\text{TQD}} = \sum_i \epsilon_i c_i^\dagger c_i + T \sum_{i,j < i} (c_i^\dagger c_j + c_j c_i^\dagger) + U \sum_{i,j < i} c_i^\dagger c_i c_j^\dagger c_j, \quad (1)$$

where  $i, j = 1, 2, 3$ , while  $c_i^\dagger$  and  $c_i$  denote the electron creation and annihilation operators of spinless electrons. The first term refers to the onsite energy  $\epsilon_i$  of an electron on dot  $i$ , for which we assume that  $\epsilon_1 = \epsilon_3 = 0$ , while  $\epsilon_2 = eV_{\text{gate}}$  can be tuned by a gate voltage. The second term describes electron tunneling between the dots, for which we assume that the tunnel matrix element  $T$  is the same for all three possible transitions. The last contribution models inter-dot Coulomb repulsion with strength  $U$ . In the present case, this term can be written in the form  $\frac{1}{2}UN(N-1)$ , where  $N$  denotes the total number of electrons on the three dots. We assume that the intra-dot interaction is practically infinite, which corresponds to modelling each dot by a single level.

In a ring-shaped geometry such as the one sketched in Fig. 1, the electrons possess two paths for travelling from the source to the drain. Thus, interference plays a role. This interference can be controlled by a magnetic flux  $\Phi$  penetrating the ring. We capture this by the replacement  $c_1^\dagger c_3 \rightarrow c_1^\dagger c_3 \exp(2\pi\Phi/\Phi_0)$ , where  $\Phi_0 = h/e$  denotes the flux quantum. Note that since we consider only spinless electrons, the effect of an associated Zeeman splitting is ignored. Nevertheless, the flux dependence of the current

provides information about the relevance of interference effects.

Dots 1 and 3 are attached to electron reservoirs with chemical potentials  $\mu_L$  and  $\mu_R$  such that the bias voltage reads  $V = \mu_L - \mu_R$ . They are fully described by

$$H_{\text{leads}} = \sum_{\ell,q} \epsilon_q c_{\ell q}^\dagger c_{\ell q} \quad (2)$$

and  $\langle c_{\ell q}^\dagger c_{\ell' q'} \rangle = f(\epsilon_q - \mu_\ell) \delta_{\ell\ell'} \delta_{qq'}$  with chemical potential  $\mu_\ell$  and the Fermi function  $f(x) = [\exp(x/k_B T) + 1]^{-1}$ . The dot-lead contact is established by the tunnel Hamiltonian

$$H_T = \sum_{\ell,q} V_{\ell q} c_{\ell q}^\dagger c_\ell + \text{h.c.} \quad (3)$$

We assume within a wide-band limit that all effective coupling strengths  $\Gamma_\ell(\epsilon) = 2\pi \sum_q |V_{\ell q}|^2 \delta(\epsilon - \epsilon_q)$  are energy independent and that the setup is symmetric such that  $\Gamma_1 = \Gamma_3 = \Gamma$ .

### 2.2. Markovian master equation

The derivation of a master equation starts from the Liouville-von Neumann equation for the full density operator,  $i\hbar\dot{R} = [H_{\text{TQD}} + H_T + H_{\text{leads}}, R]$ . By standard techniques [26], one obtains for the reduced density operator of the central system,  $\rho = \text{tr}_{\text{leads}} R$ , within second-order perturbation theory the Bloch-Redfield equation

$$\begin{aligned} \dot{\rho} &= -\frac{i}{\hbar} [H_{\text{TQD}}, \rho] - \frac{1}{\hbar^2} \text{tr}_{\text{leads}} \int_0^\infty d\tau [H_T, [\tilde{H}_T(-\tau), R]] \\ &\equiv \mathcal{L}\rho, \end{aligned} \quad (4)$$

which can be evaluated under the factorization assumption  $R = \rho_{\text{leads},0} \otimes \rho$ . The tilde denotes the interaction picture with respect to the uncoupled Hamiltonian  $H_{\text{TQD}} + H_{\text{leads}}$ ,  $\tilde{X}(t) = U_0^\dagger(t) X U_0(t)$ . We proceed by inserting the dot-lead tunnel Hamiltonian (3) and evaluate the trace over the lead states. Then we evaluate the  $\tau$ -integration, which yields a delta function and a principal value term. Neglecting the latter, we obtain the Liouvillian

$$\begin{aligned} \mathcal{L} &= -\frac{i}{\hbar} [H_{\text{TQD}}, \rho] \\ &+ \sum_{j=1,3} \frac{\Gamma_j}{\hbar} (c_j^\dagger f_j \rho c_j + c_j^\dagger \rho f_j c_j - c_j c_j^\dagger f_j \rho - \rho f_j c_j c_j^\dagger) \\ &+ \sum_{j=1,3} \frac{\Gamma_j}{\hbar} (\bar{f}_j c_j \rho c_j^\dagger + c_j \rho c_j^\dagger \bar{f}_j - c_j^\dagger \bar{f}_j c_j \rho - \rho c_j^\dagger \bar{f}_j c_j), \end{aligned} \quad (5)$$

where the index  $j$  refers to the lead to which dot  $j$  is attached and  $f_j = f(\epsilon_j + UN - \mu_j) = 1 - \bar{f}_j$ , denotes the corresponding Fermi function. Writing its argument with the operator-valued electron number  $N$  allowed us to achieve a compact notation. The solution of the master equation (5) contains the full information about the state of the central system and provides all corresponding expectation

values. However, we are interested in the statistics of the charge transported since the initial preparation, which is an expectation value of lead operators. Therefore we have to generalize the master equation formalism by introducing a counting variable which allows one to keep track of this information.

### 2.3. Full-counting statistics

The counting variable  $\chi$  is defined via the moment generating function

$$\phi(\chi, t) = \langle \exp(i\chi N_R) \rangle_t, \quad (6)$$

where  $N_R = \sum_q c_{3q}^\dagger c_{3q}$  is the electron number operator of the right lead, while the angles refer to the expectation at time  $t$ . The derivatives of  $\phi(\chi, t)$  with respect to  $i\chi$  at  $\chi = 0$  obviously are the moments of the electron distribution in the right lead,  $\langle N_R^k \rangle$ . The cumulants of the distribution are defined as the corresponding derivatives of  $\ln \phi(\chi, t)$ . For a Markov process, they eventually become linear in time. Their time-derivatives

$$C_k = \frac{\partial}{\partial t} \frac{\partial^k}{\partial (i\chi)^k} \ln \phi(\chi, t) \Big|_{\chi=0, t \rightarrow \infty} \quad (7)$$

are the current cumulants and characterize the transport. The first and the second cumulant,  $C_1$  and  $C_2$ , are essentially the stationary current  $I = eC_1$  and its zero-frequency noise  $S = e^2 C_2$ , respectively. Their ratio, the Fano factor  $F = C_2/C_1$ , represents a dimensionless measure for the noise of the transport process [27]. It is defined such that a Poissonian process corresponds to the value  $F = 1$ .

Our goal is now to find a reduced master equation that allows one to compute  $\phi(\chi, t)$ . We start again from the full density operator  $R$ , but now multiply it with the operator  $\exp(i\chi N_R)$  before tracing out the leads. This yields the generalized reduced density operator  $P(\chi, t) = \text{tr}_{\text{leads}} \{ \exp(i\chi N_R) R \}$  which contains information about the electron distribution of the drain and fulfills the trace condition  $\text{tr} P = \phi$ . Using the commutation relations  $[N_R, \Lambda] = \Lambda$  and  $[N_R, \Lambda^\dagger] = \Lambda^\dagger$ , where  $\Lambda = \sum_q V_q c_3^\dagger c_{3q}$ , we obtain the master equation

$$\dot{P}(\chi, t) = \mathcal{L}_\chi P(\chi, t) \quad (8)$$

with the augmented Liouvillian

$$\mathcal{L}_\chi = \mathcal{L} + (e^{i\chi} - 1)\mathcal{J}_+ + (e^{-i\chi} - 1)\mathcal{J}_-. \quad (9)$$

The particle current superoperators  $\mathcal{J}_\pm$  are defined via their action on the reduced density operator according to

$$\mathcal{J}_+ \rho = \frac{\Gamma_R}{2\hbar} (\bar{f}_R c_3 \rho c_3^\dagger + c_3 \rho c_3^\dagger \bar{f}_R), \quad (10)$$

$$\mathcal{J}_- \rho = \frac{\Gamma_R}{2\hbar} (c_3^\dagger f_R \rho c_3 + c_3^\dagger \rho f_R c_3). \quad (11)$$

The former superoperator describes tunneling from dot 3 to the right lead, while the latter one corresponds to the reversed process.

The dynamics of  $P(\chi, t)$  can be obtained formally by a decomposition into the eigenfunctions of  $\mathcal{L}_\chi$ . In the long-time limit, it is governed by the eigenvalue with the largest real part, denoted as  $\lambda(\chi)$ . Consequently,  $P = A(\chi) \exp[\lambda(\chi)t]$  with a normalization constant  $A(\chi)$ . For a Liouvillian with a unique stationary solution, one eigenvalue is zero, while all other eigenvalues have negative real part. Since  $\mathcal{L}_{\chi \rightarrow 0} = \mathcal{L}$ , the relevant eigenvalue is the one that fulfills  $\lambda(\chi \rightarrow 0) = 0$ . It is straightforward to see that  $\ln \phi(\chi, t) = \ln A(\chi) + \lambda(\chi)t$ . In the long-time limit, the contribution of the normalization factor is not relevant and, thus, we can conclude that  $\lambda(\chi)$  is the current cumulant generating function [23]. It can be written as the series

$$\lambda(\chi) = \sum_{k=1}^{\infty} \frac{C_k}{k!} (i\chi)^k. \quad (12)$$

The remaining task is now to compute the proper eigenvalue of  $\mathcal{L}_\chi$  and its derivatives with respect to  $\chi$ . In many cases, the reduced density matrix has a sufficiently small dimension or possesses symmetries, such that one can continue with analytical calculations. As soon as one has to resort to a numerical treatment, however, one faces the difficulty of numerically computing derivatives. This can be avoided with the recursive scheme developed in Ref. [25] even for non-Markovian master equations. Here it is sufficient to consider the Markovian limit.

The counting variable  $\chi$  can be interpreted as perturbation parameter, such that the series (12) for the eigenvalue  $\lambda(\chi)$  corresponds to the usual ansatz made in stationary perturbation theory for the eigenvalue which can be computed by the recursion [28] derived in Appendix Appendix A, see Eqs. (A.6) and (A.7). Upon setting in these expressions  $E_k = C_k/k!$ ,  $V_k = [\mathcal{J}_+ + (-1)^k \mathcal{J}_-]/k!$ , and  $P_k = |\phi_k\rangle/k!$ , we find

$$C_k = \sum_{k'=0}^{k-1} \binom{k}{k'} \text{tr} \{ \mathcal{J}_+ + (-1)^{k-k'} \mathcal{J}_- \} P_{k'}, \quad (13)$$

$$P_k = \frac{\mathcal{Q}}{\mathcal{L}} \sum_{k'=0}^{k-1} \binom{k}{k'} \{ C_{k-k'} - [\mathcal{J}_+ + (-1)^{k-k'} \mathcal{J}_-] \} P_{k'}. \quad (14)$$

The iteration starts from the stationary solution of the Liouvillian,  $P_0 = |\phi_0\rangle = \rho_\infty$ , which implies  $E_0 = C_0 = 0$ . The required multiplication with the left eigenvector  $\langle \phi_0 |$  corresponds to computing the trace. The reason for this is that the Liouvillian is trace conserving, i.e.  $\text{tr} \mathcal{L}X = 0$  for any operator  $X$ . Consequently, the projector on the subspace perpendicular to  $\rho_\infty$  reads as  $\mathcal{Q} = (\mathbf{1} - \rho_\infty \text{tr})$ . In this subspace, the Liouvillian possesses the pseudo-inverse  $\mathcal{Q}/\mathcal{L}$ . Applying it to any operator, i.e. computing  $(\mathcal{Q}/\mathcal{L})A = X$ , is equivalent to solving the linear equation  $\mathcal{L}X = A$  under the constraint  $\text{tr} X = 0$ .

In particular, we obtain for the first two cumulants, which are the current and the zero-frequency noise, the

known expressions [29]

$$I = e \operatorname{tr}(\mathcal{J}_+ - \mathcal{J}_-) \rho_\infty \quad (15)$$

$$S = e^2 \operatorname{tr}(\mathcal{J}_+ + \mathcal{J}_-) \rho_\infty - 2e^2 \operatorname{tr}(\mathcal{J}_+ - \mathcal{J}_-) \frac{Q}{\mathcal{L}} (\mathcal{J}_+ - \mathcal{J}_-) \rho_\infty. \quad (16)$$

### 3. Numerical observations

An intuitive picture for the transport properties as a function of the gate voltage can be provided for the two limiting cases in which the detuning of dot 2 is either much larger or much smaller than the inter-dot tunneling: In the limit  $|eV_{\text{gate}}| \ll T$ , all three dots are in resonance and, thus, the electrons may take with similar probability two different routes, namely  $|1\rangle \rightarrow |3\rangle$  and  $|1\rangle \rightarrow |2\rangle \rightarrow |3\rangle$ . Therefore one expects interference to be relevant and, thus, the current should depend on the flux penetrating the ring. If the gate voltage is large, by contrast, i.e. for  $|eV_{\text{gate}}| \gg T$ , dot 2 is off-resonant and, thus, should be of minor relevance. Therefore, the transport properties of the setup are expected to be essentially those of a double quantum dot formed by dots 1 and 3. Our numerical results, however, will demonstrate that this is only true for the average current, while the current noise is significantly altered by the presence of dot 2 even when far detuned.

As a first step, we solve the master equation numerically. In doing so, we identify parameter regimes in which the stationary state of the triple dot is dominated by a few eigenstates. This allows us to reduce the complexity of the master equation, such that we can achieve an analytical treatment that provides insight to the transport mechanism. For the numerical solution, we use the dot-lead coupling  $\Gamma$  as energy unit. For the typical value  $\Gamma = 10\mu\text{eV}$ , the corresponding current unit reads  $e\Gamma/\hbar = 2.43\text{nA}$ .

#### 3.1. Stationary current and occupation probabilities

The stationary current as a function of the gate voltage  $V_{\text{gate}} = \epsilon_2/e$  is shown in Fig. 3. It demonstrates that for  $|\epsilon_2| \lesssim T$ , the current indeed is significantly flux dependent as conjectured above. For flux  $\Phi = 0$ , the currents assumes its minimum. This can be explained by the fact that then, the state  $|\psi_{\text{dark}}\rangle = (|1\rangle - |2\rangle)/\sqrt{2}$  is an eigenstate of the triple dot Hamiltonian and is orthogonal to state  $|3\rangle$ . Therefore it is not directly coupled to the right lead, which has the consequence that  $|\psi_{\text{dark}}\rangle$  may trap an electron and thereby enhance Coulomb blockade [30].

For a systematic investigation of the importance of interference, we computed the visibility

$$\nu = \frac{I_{\text{max}} - I_{\text{min}}}{I_{\text{max}} + I_{\text{min}}}, \quad (17)$$

where  $I_{\text{max}} = \max_{\Phi} I(\Phi)$  is the maximal current for a given gate voltage, and  $I_{\text{min}}$  is defined accordingly. The inset of Fig. 2 demonstrates that for  $|\epsilon_2| \gg T$ , interference plays a minor role. The reason for this is that when dot 2 is

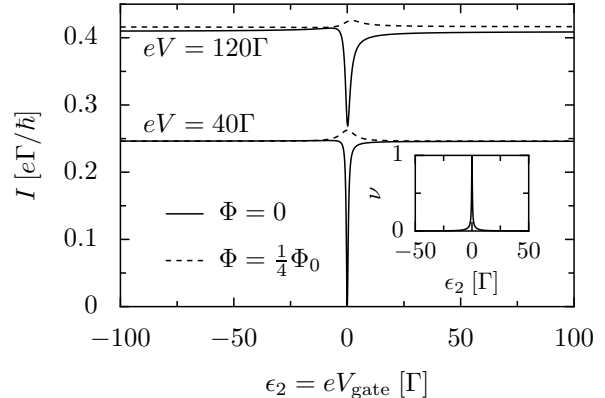


Figure 2: Current as a function of the gate voltage  $V_{\text{gate}} = \epsilon_2/e$  for different magnetic fluxes and bias voltages which are applied symmetrically such that  $\mu_L = -\mu_R = V/2$ . The inter-dot tunnel coupling and interaction are  $T = 2\Gamma$  and  $U = 40\Gamma$ , respectively. Inset: Corresponding visibility.

strongly detuned, transport through this off-resonant dot requires co-tunneling and, thus, the path via dot 2 has a significantly lower probability than the direct path.

Henceforth we focus on the region *without* interference effects. There a main feature of the current is that it exhibits plateaus, see Fig. 3(a). This is consistent with the usual Coulomb blockade scenario in which the bias and the gate voltage, determine the maximal number electrons that can reside on the dots. Accordingly, the probability for having a particular dot occupation changes at the steps, as can be appreciated from Fig. 3(b). Moreover, an electron can tunnel from the left lead to dot 1 only if it has sufficient energy to compensate the Coulomb repulsion of the electrons that are already in the triple quantum dot. Thus the occupation with  $N > 0$  electrons is possible only if the chemical potential is larger than  $(N - 1)U$ . For the symmetric positive voltage drop assumed herein,  $\mu_L = e|V|/2$ . This implies that the occupation probability  $p_N$  vanishes for all  $N > 1 + e|V|/2U$ , which is consistent with the occurrence of the steps shown in Fig. 3(b). In particular, for  $e|V| < 2U$ , only single occupation plays a role. Below we will use this fact for establishing an analytical treatment in the low-bias regime.

#### 3.2. Shot noise and Fano factor

So far we have seen that unless the voltage is extremely low, the current is always of the order  $e\Gamma/\hbar$ , i.e. the gate voltage and the bias voltage modify the current merely by a factor of the order unity. Figure 4 demonstrates that the noise, characterized by the Fano factor  $F = S/e|I|$ , possesses a more sensitive voltage dependence. In particular in the single-electron regime, the Fano factor possesses a quadratic dependence on  $\epsilon_2$  (upper inset of Fig. 4) and can assume values that are several order of magnitude above the Poissonian value  $F = 1$ . This already indicates electron bunching, where each bunch of electrons has charge  $eF$  [31].

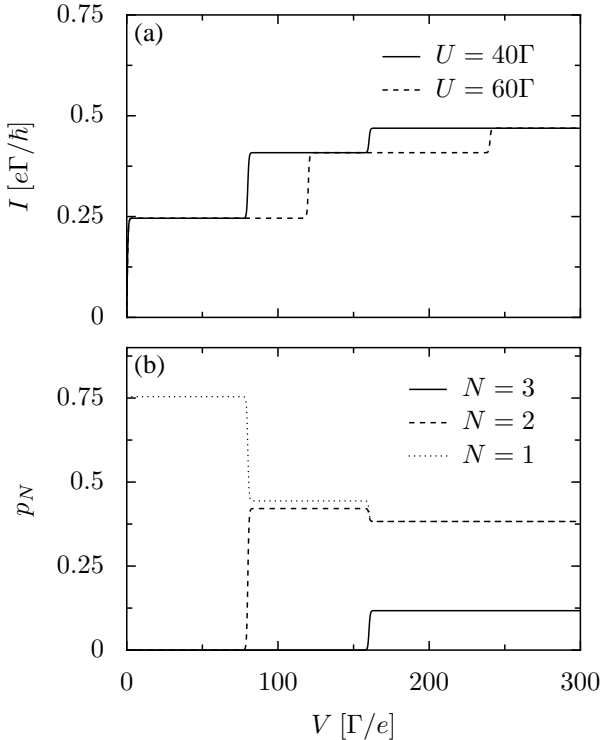


Figure 3: (a) Current as a function of the bias voltage  $V = \mu_L - \mu_R$  for various interaction strengths. The inter-dot tunnel coupling and the gate voltage are  $T = 2\Gamma$  and  $V_{\text{gate}} = \epsilon_2/e = 40\Gamma/e$ , respectively. (b) Probability that for  $U = 40\Gamma$ , the asymptotic state of the triple quantum dot contains  $N$  electrons.

In the two-electron regime, i.e. for bias voltages in the range  $U/2e < V < U/e$ , the Fano factor (lower inset of Fig. 4) exhibits a quadratic dependence on  $\epsilon_2$  as well, but the absolute values are now significantly smaller. In the three-electron regime, i.e. for  $eV > 2U$ , the Fano factor is close to unity and almost independent of  $\epsilon_2$ . This indicates a Poissonian transport process. Since the bunching effects are most pronounced in the low-bias regime in which at most one electron can reside on the triple dot.

### 3.3. Full counting statistics

The huge values of the Fano factor discussed above indicate that the current is formed by fairly independent avalanches whose charge on average is  $q = eF$ . A decisive criterion can only be the full time-dependent distribution function of the transported electrons. This is equivalent to the frequency-dependent full-counting statistics or the time-evolution of all cumulants. Here we restrict ourselves to the corresponding long-time limit which provides the information about the low-frequency fluctuations.

Provided that the avalanches are completely uncorrelated and their duration is practically zero, the cumulants (7) should read [32, 31]

$$C_k = \frac{e\Gamma}{\hbar} \left(\frac{q}{e}\right)^k. \quad (18)$$

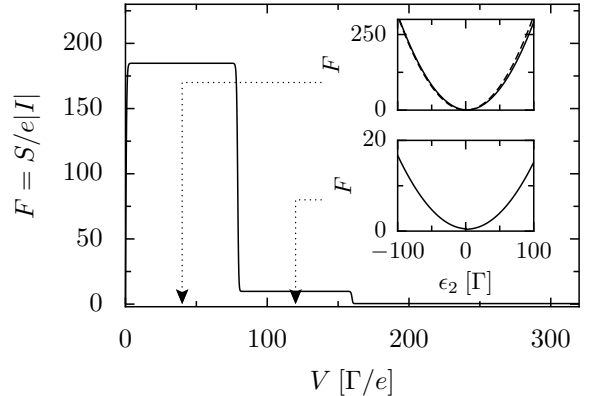


Figure 4: Fano factor of the current shown in Fig. 3 for the interaction strength  $U = 40\Gamma$ . Insets: Fano factor as a function of the detuning  $\epsilon_2 = eV_{\text{gate}}$  for the bias voltages  $V = 40\Gamma/e$  and  $V = 120\Gamma/e$ , which correspond to values from the first and the second plateau, respectively, as indicated by the arrows. The dashed line in the upper inset marks the analytical result derived in Section 4. It is barely distinguishable from the numerical result.

Figure 5 demonstrates that the  $C_k$  as a function of the order  $k$  indeed grow exponentially fast in both the one-electron regime and the two-electron regime. The solid line in Fig. 5, however, demonstrates that only the cumulants of low order follow this behavior, while those of higher order assume significantly larger absolute values and some even become negative. The closer investigation of the data reveals that already the third cumulant deviates from conjecture (18).

## 4. Analytical solution in the one-electron regime

If the bias voltage is so small that only one electron can reside on the triple dot, i.e. for  $eV < 2U$ , all relevant eigenstates of  $H_{\text{TQD}}$  are the empty state  $|0\rangle$  and the one-electron states. To lowest order in  $T/\epsilon_2$  the latter read

$$|\phi_1\rangle = \frac{1}{\sqrt{2}} (|1\rangle - |3\rangle), \quad (19)$$

$$|\phi_2\rangle = \frac{1}{\sqrt{2}} (|1\rangle + |3\rangle), \quad (20)$$

$$|\phi_3\rangle = \frac{1}{\sqrt{\epsilon_2^2 + 2T^2}} (T|1\rangle + \epsilon_2|2\rangle + T|3\rangle), \quad (21)$$

where the localized states  $|j\rangle = c_j^\dagger|0\rangle$  are used as basis. For symmetry reasons, each of these states couples with equal strength to the left and to the right lead, such that the corresponding incoherent transition rates are given by

$$\Gamma_{L,n} = \Gamma_{R,n} = \Gamma |\langle \phi_n | 3 \rangle|^2 \equiv \Gamma_n. \quad (22)$$

For the approximative eigenstates (19)–(21) the coupling constants read  $\Gamma_1 = \Gamma_2 = \Gamma/2$  and  $\Gamma_3 = \Gamma T^2/\epsilon_2^2$ .

If the dot-lead coupling  $\Gamma$  is sufficiently small, one can neglect within a rotating-wave approximation off-diagonal

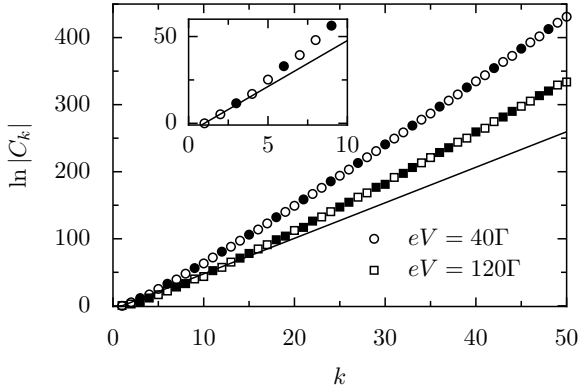


Figure 5: Full counting statistics of the current for  $\epsilon_2 = 100\Gamma$  and the bias voltages  $V = 40\Gamma/e$  (one-electron regime) and  $V = 120\Gamma/e$  (two-electron regime) expressed by the cumulants  $C_k$ . All other parameters are as in Fig. 4. Open symbols marks positive values while filled symbols correspond to negative values. The line marks the values for uncorrelated tunneling of charges  $q = eF$  in the one-electron regime (circles), cf. Eq. (18). Inset: Enlargement of the lower left corner.

elements of the reduced density operator [10], such that the system is well described by the occupation probabilities  $(P_0, P_1, P_2, P_3)$  for the states  $|0\rangle$  and  $|\phi_n\rangle$ ,  $n = 1, 2, 3$ . The corresponding Liouville operator is

$$\mathcal{L}_{1e} = \begin{pmatrix} -\Gamma & \Gamma_1 & \Gamma_2 & \Gamma_3 \\ \Gamma_1 & -\Gamma_1 & 0 & 0 \\ \Gamma_2 & 0 & -\Gamma_2 & 0 \\ \Gamma_3 & 0 & 0 & -\Gamma_3 \end{pmatrix}, \quad (23)$$

where the index “1e” refers to the restriction to single occupation. We have used the sum rule  $\Gamma = \sum_{n=1}^3 \Gamma_n$  which follows from the completeness relation for the (exact) eigenstates  $|\phi_n\rangle$  in the one-electron subspace. The corresponding particle current operators are  $\mathcal{J}_- = 0$ , while  $\mathcal{J}_+$  is obtained from  $\mathcal{L}_{1e}$  by keeping only the elements placed above the diagonal.

The stationary state of the Liouville operator can now be readily computed and reads  $P_0 = 1/4 = P_n$  for all  $n$ , which implies  $\langle n_3 \rangle = 1/4$ . Inserting this into the current formula (15), yields  $I = e\Gamma/4\hbar$ . Notice that the second term of the current formula vanishes. Interestingly enough, the current does not depend on the structure of the eigenstates, which is a consequence of the mentioned sum rule for the  $\Gamma_n$ .

For the Liouville operator (23), not only the stationary current, but also the zero-frequency noise (16) can be evaluated exactly. Starting from that expression, one obtains after some lines of straightforward calculation the result

$$S = \frac{e^2}{32\hbar} \sum_{n,n'=1}^3 \frac{\Gamma_n^2}{\Gamma_{n'}} + \frac{e^2}{16\hbar} \sum_{n=1}^3 \frac{\Gamma_1\Gamma_2\Gamma_3}{\Gamma_n^2}. \quad (24)$$

In the limit  $\Gamma_{1,2} \ll \Gamma_3$ , only terms with  $\Gamma_3$  in the denominator are relevant, so that we obtain  $S = \Gamma^2/32\Gamma_3$ . With

the above expressions for  $\Gamma_n$ , the corresponding Fano factor becomes

$$F_{1e} = \frac{\epsilon_2^2}{8T^2}. \quad (25)$$

It indeed exhibits the predicted parabolic dependence on the gate voltage  $V_{\text{gate}} = \epsilon_2/e$ . A quantitative comparison of both the current and the Fano factor with the numerical results depicted in the upper inset of Fig. 4 yields a satisfactory agreement in the range considered here. This implies that our one-electron model indeed captures the essential features of the electron avalanches through the triple quantum dot. Moreover, it implies that the (average) size of the avalanches is  $q = e\epsilon_2^2/8T^2$ .

The proportionality of the Fano factor to  $(\epsilon_2/T)^2$  suggests for the transport in the one-electron regime the following scenario: Assume that the off-resonant dot is initially unoccupied, while electrons are transported via dots 1 and 3. Then, according to standard perturbation theory, electrons in these dots may tunnel to dot 2 with a probability amplitude proportional to the tunnel matrix element divided by the energy difference, i.e. with a probability  $p \propto (T/\epsilon_2)^2$ . Thus after on average  $1/p$  electrons have been transported, an electron will tunnel to dot 2 and cause temporary Coulomb blockade which is resolved only when the electron tunnels out. Thus, the dynamics is given by periods with an open channel that on average terminate after an avalanche with  $1/p \propto (T/\epsilon)^2$  electrons has been transported, which explains the observed proportionality of the Fano factor  $F \propto (\epsilon_2/T)^2$ . This scenario also explains why the numerically found cumulants deviate from conjecture (18): The average duration of an avalanche is as long as the waiting time between subsequent avalanches, while conjecture (18) is based on the assumption of a short avalanche duration.

In the limit  $\Gamma_3 \ll \Gamma$ , it is still possible to evaluate some cumulants of higher order analytically, although this becomes increasingly tedious. Nevertheless it is worth proceeding up to fourth order for which we obtain

$$C_1 = \frac{\Gamma}{4\hbar}, \quad (26)$$

$$C_2 = \frac{\Gamma}{4\hbar} \left( \frac{\Gamma}{8\Gamma_3} \right), \quad (27)$$

$$C_3 = -\frac{3\Gamma}{4\hbar} \left( \frac{\Gamma}{8\Gamma_3} \right)^2, \quad (28)$$

$$C_4 = \frac{3\Gamma}{4\hbar} \left( \frac{\Gamma}{8\Gamma_3} \right)^3. \quad (29)$$

Thus, the first two cumulants behave as expected for short avalanches with charge  $q = e\Gamma/8\Gamma_3$ . However, already the third and the fourth cumulant deviate from the Poissonian value by a factor  $\pm 3$ .

## 5. Conclusions

The emergence of an interference pattern with good visibility usually requires the coherent superposition of two

or more paths that are traversed with appreciable probability. In an Aharonov-Bohm interferometer formed by quantum dots in ring configuration, a significant detuning of only one dot has the consequence that transport through the associated path requires co-tunneling. Since this reduces the transmission probability of that path, the interference pattern as a function of a penetrating flux will fade out. We have demonstrated that, nevertheless, strongly detuned setups of that type bear interesting effects manifest in the noise properties of the current. In particular, we have shown that strong electron bunching may occur. It turned out that this is most pronounced in the low bias regime in which Coulomb repulsion forbids the occupation of the triple quantum dot by more than one electron.

The prime quantity of interest in that context is the Fano factor for which we have predicted huge values: the noise can exceed the level set by the Schottky formula by several orders of magnitude. The physical reason for this is that electrons may become trapped in the off-resonant quantum dot, such that Coulomb blockade interrupts the transport until the trapped electron leaves the interferometer. The analysis of the higher-order charge fluctuations—the full-counting statistics—revealed that the cumulants grow exponentially with their order. This leads us to the conclusion that the current consists of avalanches with a finite duration.

For the computation of the full-counting statistics, we have employed the iterative scheme recently developed in Ref. [25]. This was essential for the treatment of the full many-electron problem, since the Hilbert space of our model was already too large for a full analytical treatment. In the most relevant regime of single occupation, it was also possible to perform the first iteration steps analytically and, thus, we obtained expressions for the first four cumulants in the limit of strong detuning and low voltage bias.

In conclusion, we have studied electron interferometers in a regime that so far has not attracted much attention most likely due to the lack of pronounced interference effects. Precisely in this regime, however, the shot noise properties are most interesting and strong electron bunching occurs. Thus, quantum dots in ring configuration may serve not only for the observation of interference effects, but also for the creation of currents with widely tunable super-Poissonian fluctuations.

## Acknowledgements

This work has been supported by the Spanish project MAT2008-02626 and by a Ramón y Cajal fellowship (S.K.). F.D. acknowledges financial support by MEC (Spain) through a FPI grant.

## Appendix A. Rayleigh-Schrödinger perturbation theory

In most textbooks on quantum mechanics, perturbation theory is formulated for a perturbation linear in the small parameter, while in  $\mathcal{L}_\chi$  contains arbitrarily high powers of  $\chi$ . In this appendix we derive a recursive scheme for the representation of an eigenvalue as a Taylor series in a perturbation parameter. Our calculation is inspired by Chap. 5 of Ref. [28]. Despite the fact that we formulate the problem in terms of a quantum mechanical energy eigenvalue problem, our derivation is not restricted to Hermitian operators.

We consider a “Hamiltonian”  $H = H_0 + V(\alpha)$  for which the perturbation  $V(\alpha)$  is an analytical function of the perturbation parameter  $\alpha$  and vanishes in the limit  $\alpha \rightarrow 0$ . Thus, it can be decomposed into the series

$$V(\alpha) = \sum_{k=1}^{\infty} \alpha^k V_k. \quad (\text{A.1})$$

Our goal is to find a series for the eigenvalue  $E(\alpha)$  of  $H$  that fulfills  $\lim_{\alpha \rightarrow 0} E(\alpha) = E_0$ , where  $E_0$  is the eigenvalue of  $H_0$  corresponding to a particular eigenvector  $|\phi_0\rangle$ , i.e.,  $H_0|\phi_0\rangle = E_0|\phi_0\rangle$ . A central assumption is that both the eigenvalue and the eigenvector  $|\phi(\alpha)\rangle$  can be decomposed into a series in  $\alpha$  as well, such that we can employ the ansatz

$$E(\alpha) = E_0 + \sum_{k=1}^{\infty} \alpha^k E_k, \quad (\text{A.2})$$

$$|\phi(\alpha)\rangle = |\phi_0\rangle + \sum_{k=1}^{\infty} \alpha^k |\phi_k\rangle. \quad (\text{A.3})$$

For the present purpose, it is sufficient to consider only the case of non-degenerate  $E_0$ . Note that for non-Hermitian  $H_0$ ,  $\langle\phi_0|$  is generally not the Hermitian adjoint of  $|\phi_0\rangle$ , but rather the corresponding left eigenvector, i.e., the solution of  $\langle\phi_0|H_0 = E_0\langle\phi_0|$ . We choose the normalization such that  $\langle\phi_0|\phi_0\rangle = 1$ .

We start by writing the eigenvalue equation  $H|\phi(\alpha)\rangle = E(\alpha)|\phi(\alpha)\rangle$  in the form

$$(H_0 - E_0)|\phi(\alpha)\rangle = \{E(\alpha) - E_0 - V(\alpha)\}|\phi(\alpha)\rangle, \quad (\text{A.4})$$

which is convenient for the derivation of a formal solution and subsequent iteration. Since  $(H_0 - E_0)|\phi_0\rangle = 0$ , Eq. (A.4) defines  $|\phi(\alpha)\rangle$  only up to a component proportional to  $|\phi_0\rangle$ . Moreover, this implies that the inverse of  $H_0 - E_0$  does not exist. It is however possible to define the pseudo-inverse  $Q(H_0 - E_0)^{-1}Q$  [or in short:  $Q/(H_0 - E_0)$ ], where  $Q$  is the projector on the subspace spanned by the eigenvectors of  $H_0$  with non-zero eigenvalue. In the present case of non-degenerate  $E_0$ , it reads  $Q = \mathbf{1} - |\phi_0\rangle\langle\phi_0|$ .

The pseudo-inverse allows one to cast Eq. (A.4) into the form

$$|\phi(\alpha)\rangle = |\phi_0\rangle + \frac{Q}{H_0 - E_0} \{E(\alpha) - E_0 - V(\alpha)\}|\phi(\alpha)\rangle. \quad (\text{A.5})$$

The first term on the right-hand side can be multiplied by any factor without violating compliance with Eq. (A.4). We have chosen it such that  $\lim_{\alpha \rightarrow 0} |\phi(\alpha)\rangle = |\phi_0\rangle$ . Moreover, since  $\langle \phi_0 | Q = 0$ , the relation  $\langle \phi_0 | \phi(\alpha)\rangle = \langle \phi_0 | \phi_0\rangle = 1$  holds. An important feature of Eq. (A.5) is that the operator on the right-hand side is of first order in  $\alpha$ . Therefore, it can be solved iteratively in the following way.

Multiplying Eq. (A.4) by  $\langle \phi_0 |$ , its left-hand-side vanishes owing to  $\langle \phi_0 | H_0 = E_0 \langle \phi_0 |$ . Thus we obtain  $E(\alpha) - E_0 = \langle \phi_0 | V(\alpha) | \phi(\alpha)\rangle$ . We then insert for  $E(\alpha)$ ,  $V(\alpha)$ , and  $|\phi(\alpha)\rangle$  the series (A.1)–(A.3) and compare the coefficients to obtain the  $k$ th-order energy shift

$$E_k = \sum_{k'=1}^k \langle \phi_0 | V_{k'} | \phi_{k-k'}\rangle. \quad (\text{A.6})$$

It depends on the still unknown correction of the eigenvector,  $|\phi_{k-k'}\rangle$ , which we determine from Eq. (A.5). We again insert Eqs. (A.1)–(A.3) and compare coefficients to find

$$|\phi_k\rangle = \frac{Q}{H_0 - E_0} \left\{ \sum_{k'=1}^{k-1} E_{k'} |\phi_{k-k'}\rangle - \sum_{k'=1}^k V_{k'} |\phi_{k-k'}\rangle \right\}. \quad (\text{A.7})$$

Equations (A.6) and (A.7) allow the recursive computation of the series (A.2) for the eigenvalue shift  $E(\alpha)$ .

## References

- [1] R. P. Feynman, Eng. Sci. 23 (1960) 22, lecture given at the APS meeting 1959, see <http://www.its.caltech.edu/~feynman/plenty.html>.
- [2] J. C. Ellenbogen, J. C. Love, Proc. IEEE 88 (2000) 386.
- [3] P. Hänggi, M. Ratner, S. Yaliraki, Chem. Phys. 281 (2002) 111–502.
- [4] G. Cuniberti, G. Fagas, K. Richter (Eds.), Molecular Electronics, Lecture Notes in Physics, Springer, Berlin, 2005.
- [5] F. Grossmann, T. Dittrich, P. Jung, P. Hänggi, Phys. Rev. Lett. 67 (1991) 516.
- [6] C. E. Creffield, G. Platero, Phys. Rev. B 65 (2002) 113304.
- [7] J. Lehmann, S. Camalet, S. Kohler, P. Hänggi, Chem. Phys. Lett. 368 (2003) 282.
- [8] S. Camalet, J. Lehmann, S. Kohler, P. Hänggi, Phys. Rev. Lett. 90 (2003) 210602.
- [9] G. Platero, R. Aguado, Phys. Rep. 395 (2004) 1.
- [10] S. Kohler, J. Lehmann, P. Hänggi, Phys. Rep. 406 (2005) 379.
- [11] N. C. van der Vaart, S. F. Godijn, Y. V. Nazarov, C. J. P. M. Harmans, J. E. Mooij, Phys. Rev. Lett. 74 (1995) 4702.
- [12] R. H. Blick, R. J. Haug, J. Weis, D. Pfannkuche, K. von Klitzing, K. Eberl, Phys. Rev. B 53 (1996) 7899.
- [13] W. G. van der Wiel, S. De Franceschi, J. M. Elzerman, T. Fujisawa, S. Tarucha, L. P. Kouwenhoven, Rev. Mod. Phys. 75 (2003) 1.
- [14] D. Schröer, A. D. Greentree, L. Gaudreau, K. Eberl, L. C. L. Hollenberg, J. P. Kotthaus, S. Ludwig, Phys. Rev. B 76 (2007) 075306.
- [15] L. Gaudreau, S. A. Studenikin, A. S. Sachrajda, P. Zawadzki, A. Kam, J. Lapointe, M. Korkusinski, P. Hawrylak, Phys. Rev. Lett. 97 (2006) 036807.
- [16] M. C. Rogge, R. J. Haug, Phys. Rev. B 77 (2008) 193306.
- [17] S. Gustavsson, M. Studer, R. Leturcq, T. Ihn, K. Ensslin, D. C. Driscoll, A. C. Gossard, Phys. Rev. Lett. 99 (2007) 206804.
- [18] B. Michaelis, C. Emary, C. W. J. Beenakker, Europhys. Lett. 73 (2006) 677.
- [19] C. Pörtl, C. Emary, T. Brandes, Phys. Rev. B 80 (2009) 115313.
- [20] R. Sanchez, E. Cota, R. Aguado, G. Platero, Phys. Rev. B 74 (2006) 035326.
- [21] M. Busl, R. Sánchez, G. Platero, arXiv:0907.0182 [cond-mat].
- [22] G. B. Lesovik, L. S. Levitov, Phys. Rev. Lett. 72 (1994) 538.
- [23] D. A. Bagrets, Yu. V. Nazarov, Phys. Rev. B 67 (2003) 085316.
- [24] W. Belzig, Phys. Rev. B 71 (2005) 161301(R).
- [25] C. Flindt, T. Novotný, A. Braggio, M. Sasseti, A.-P. Jauho, Phys. Rev. Lett. 100 (2008) 150601.
- [26] K. Blum, Density Matrix Theory and Applications, 2nd Edition, Springer, New York, 1996.
- [27] U. Fano, Phys. Rev. 72 (1947) 26.
- [28] J. J. Sakurai, Modern Quantum Mechanics, 2nd Edition, Addison-Wesley, Reading, 1995.
- [29] C. Flindt, T. Novotný, A.-P. Jauho, Phys. Rev. B 70 (2004) 205334.
- [30] C. Emary, Phys. Rev. B 76 (2007) 245319.
- [31] L. S. Levitov, M. Reznikov, Phys. Rev. B 70 (2004) 115305.
- [32] N. G. van Kampen, Stochastic processes in physics and chemistry, North-Holland, Amsterdam, 1992.